

Impact of QED/EW corrections on m_W measurement:

how to reach precision for QED FSR using PHOTOS

Z. Was*

* IFJ PAN, 31342 Krakow, Poland

Plan (modified in the last moment toward how to estimate systematic errors):

1. Why bother: precision of leptonic variables. **1a.** → **Main issues** → **missing effects, matching genuine weak and lineshape.** Eight talks in collision
2. Phase-space, original event de-construction.
3. Toward Poissonian distribution for tangent-space of “independent” photons.
4. Matrix elements in use.
5. Event record.
6. Factorization of production, Mustraal-frame. Works of Mirkes and Kleiss
7. Factorization of Genuine Weak Effects: work of D. Bardin team members.
8. QED initial-final state interference.

9. Tests and validations. **10. → Summary and outlook.**

1. Photos is one of the MC project which relies on additional symmetries present in Fied Theory results:
 - (a) conformal symmetry of subset of QED for additional photons (no pairs)
 - (b) closely related with that sub-group (sub-representation) structure of *layers* for massless and massive representations of Lorentz group and similar for gauge symmetry groups.
2. It is fantastic how parts of exact spin amplitudes can be separated into parts accordingly to gauge invariance;
3. their **future** role to define LL NLL terms etc appear as a bonus, not necessarily the original demand.
4. Despite being used for QED MC they are barely used elsewhere. Work of Yennie Frautchi Suura waits to be extended?
5. Anyway all this defines scheme of how to evaluate systematic errors and how to improve.

1. Phase space
2. Then matrix elements re-ordering: to a form of parts: $\beta_0, \beta_1, \beta_2$ of YFS
3. This was and *is* important for Photos; its iteration algorithms was developped simultaneously with the work on matrix elements for $e^+e^- \rightarrow Z \rightarrow \mu^+\mu^-2(3)\gamma$ processes.
4. Definition of the quantum state for the intermediate (decaying) object.
5. Future improvements:
 - (a) Mustraal Frame is direction for the progress
 - (b) Missing effects like IFI interference
 - (c) Tests
 - (d) User: to be reproduced benchmarks
6. **That is what I want to cover in my talk (at least in part).**

1. Why bother: precision of leptonic variables.

5

1. Lepton directions are the most precise measured quantities at LHC detectors.
2. Lepton energies are much better measured than energies or directions of hadronic jets.
3. Observables which can take that into account are thus of the highest interest for any precision physics goals.
4. Bremsstrahlung affects direction and energy of outgoing leptons.
5. **That is the reason behind simulation tools for the related phenomena.**
6. Also: can such things be treated/simulated separately or must it remain inseparable part of the complete predictions.

Presentation, practical aspects

- PHOTOS (by E.Barberio, B. van Eijk, Z. W., P.Golonka) is used to simulate the effect of radiative corrections in decays, since 1989.
- Full events combining complicated tree structure of production and subsequent decays are fed into PHOTOS, with the help of HEPEVT event record of F77
- PHOTOS C++ version for HepMC event record: Photospp
- At every branching of event tree, PHOTOS intervene. With certain probability extra photon(s) are added and kinematics of other particles adjusted.
- PHOTOS algorithm is iterative. First over emitters; interference (or matrix element) weight is used. Iteration over consecutive emissions is external.
- Compatibility with exponentiation and resummation of collinear terms at the same time.

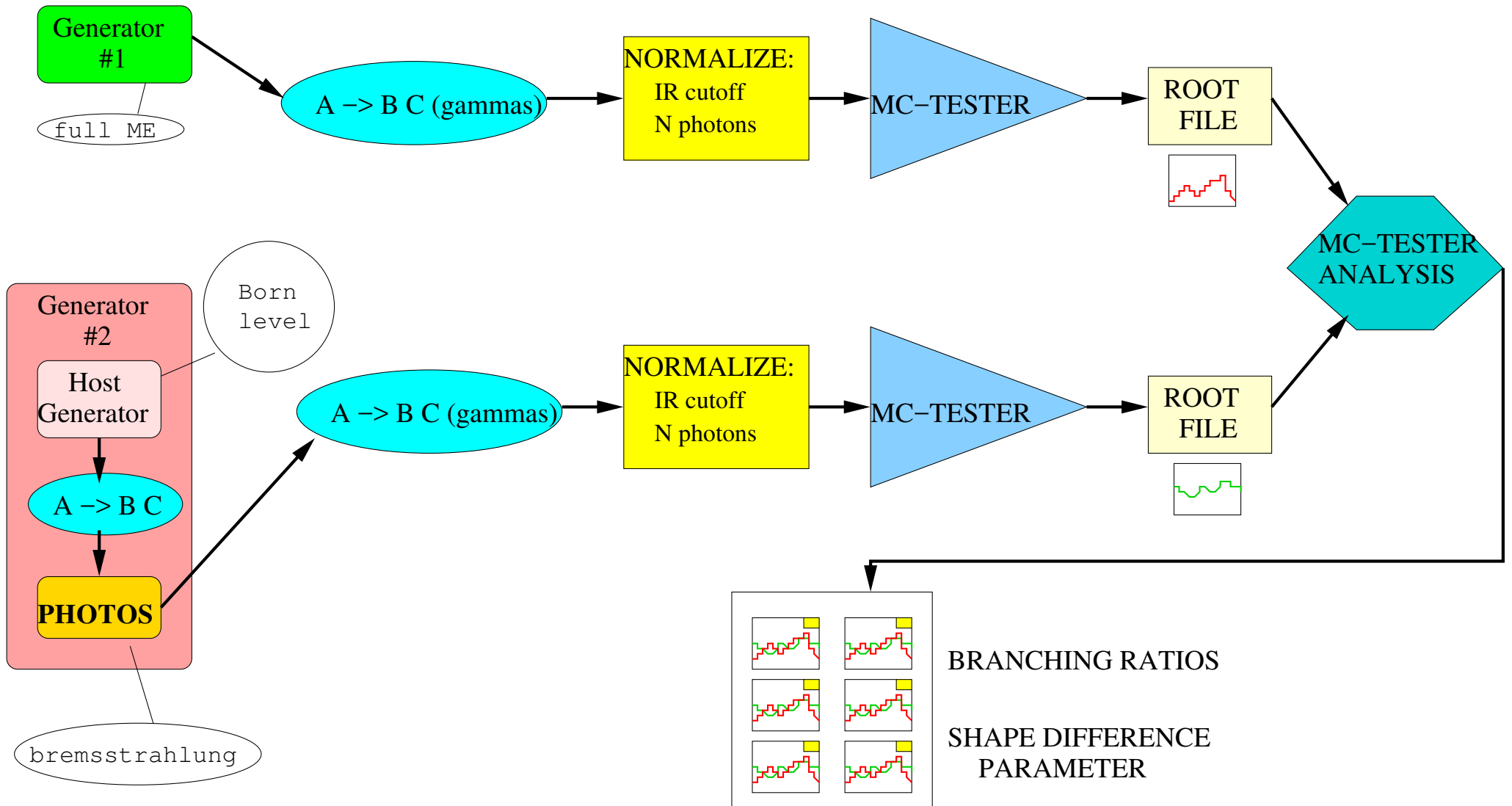
Main References

- E. Barberio, B. van Eijk and Z. Was, Comput. Phys. Commun. **66**, 115 (1991): **single emission**
- E. Barberio and Z. Was, Comput. Phys. Commun. **79**, 291 (1994). **double emission introduced, tests with second order matrix elements**
- P. Golonka and Z. Was, EPJC 45 (2006) 97 **multiple photon emission introduced, tests with precision second order exponentiation MC.**
- P. Golonka and Z. Was, EPJC 50 (2007) 53 **complete QED ME in Z decay**
- G. Nanava, Z. Was, Eur.Phys.J.C51:569-583,2007, **best description of phase space**
- G. Nanava, Z. Was, Q. Xu, Eur.Phys.J.C70:673,2010. **complete QED ME in W decay**
- N. Davidson, T. Przedzinski, Z. Was, Comput. Phys. Commun. 199 (2016) 86, **HepMC interface ME in W, Z decays, light lepton pair emission.**
- S. Antropov et al. Acta Phys.Polon. B48 (2017) 1469 **tests light lepton pair emission.**

- KKMC - second order ME., FSR (Final State Radiation), with CEEX exp.
- KKMC O(1)EXP - first order matrix element, FSR only, also with CEEX exponentiation
- KoralZ O(1) - fixed first order FSR, no exponentiation, n
- KORALZ - "pragmatic" second order FSR, with EEX exponentiation
- PHOTOS O(1) - standard option of single photon emission in PHOTOS,
- PHOTOS O(2) - standard option of double photon emission in PHOTOS,
- PHOTOS O(3) - up to triple photon emission, accordingly to the same scheme, as above
- PHOTOS O(4) - up to quatic photon emission, accordingly to the same scheme, as above
- PHOTOS EXP - multiphoton
- PHOTOS EXP + multiphoton kernel based on matrix element 2007
- PHOTOS EXP + multiphoton kernel based on matrix element+ emission of pairs (2016)
- TAUOLA O(1) - fixed first order FSR in tau decays, no exponentiation, as published in CPC

- Each pair of the programs results was compared in a semi automated way as it was representing 20+ plots and tables of results as well.
- with the help of comparisons one could address:
- question of technical precision
- question of physics precision for a class of effects which wa switched on or off.
- It was always expected that such comparisons **will be repeated by the users** for the experimental conditions of importance.
- automated generated plots of 2005 require attentive looks.
- some options are for comparisons with electroweak calculations, to check if separating-out of QED from fixed order calculatio is consistent with choice for PHOTOS.
- such scheme leaves for separate discussion question of IFI interference

MC-TESTER to test PHOTOS/TAUOLA



Found decay modes:

Decay channel	Branching Ratio \pm Rough Errors		Max. shape dif. param.
	Generator #1	Generator #2	
$Z^0 \rightarrow \mu^- \mu^+ \gamma$	14.8164 \pm 0.0038%	14.8059 \pm 0.0038%	0.00003
$Z^0 \rightarrow \mu^- \mu^+$	83.9177 \pm 0.0092%	83.9314 \pm 0.0092%	0.00000
$Z^0 \rightarrow \mu^- \mu^+ \gamma \gamma$	1.2659 \pm 0.0011%	1.2626 \pm 0.0011%	0.00960

Similarity coefficients: T1=0.027067 %, T2=0.011286 %

- As we see agreement is perfect
- The systematic error for FSR originates from non included terms...
- ... that is: (i) IFI (ii) event record definition of intermediate decaying state

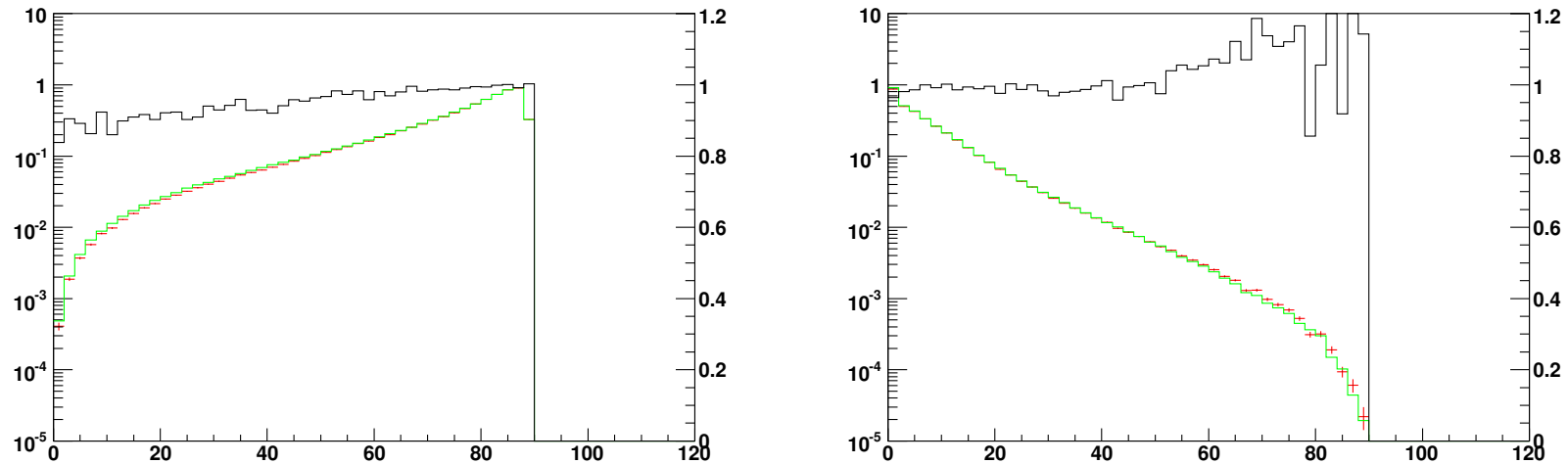


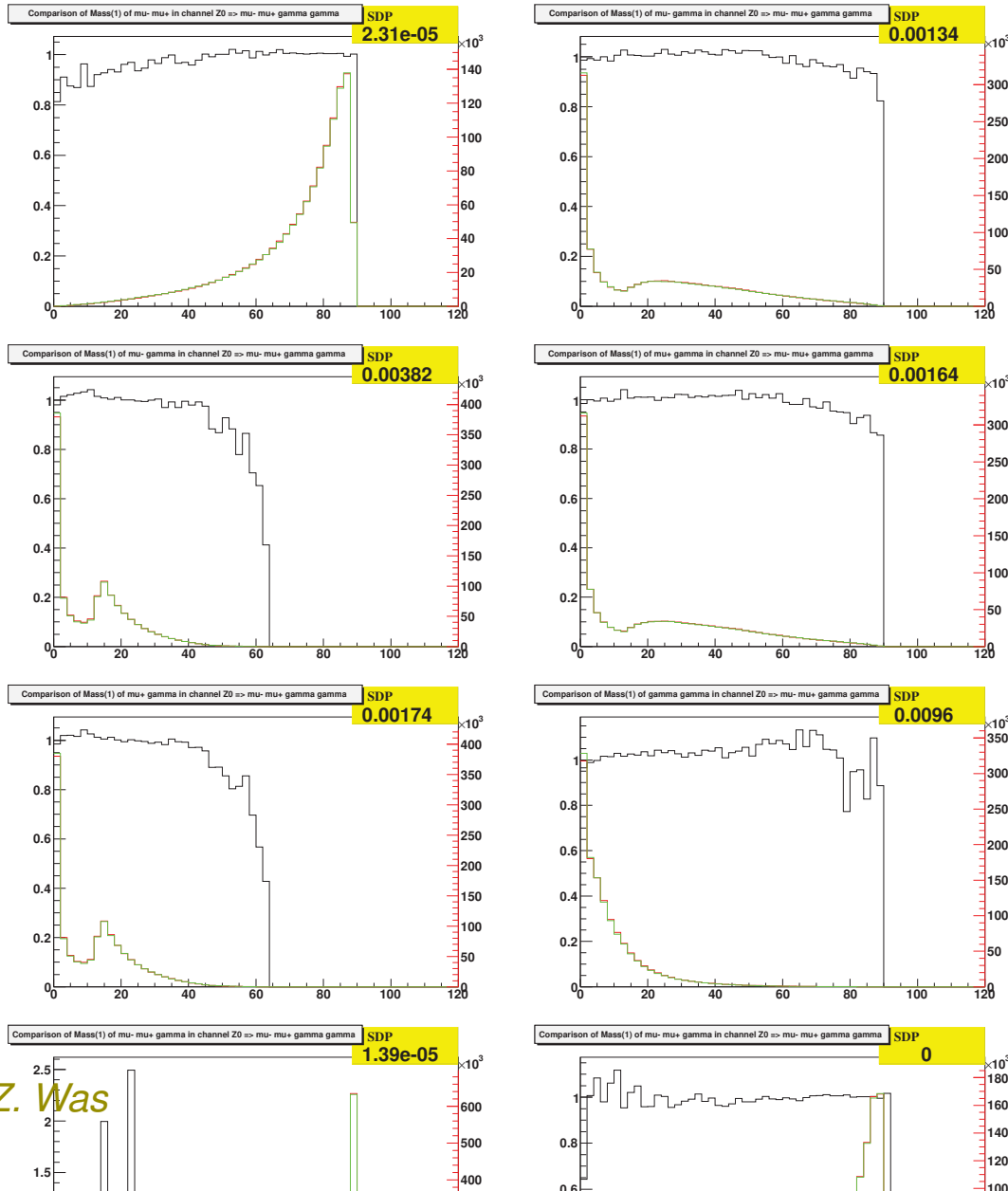
Figure 6: Comparisons of improved PHOTOS with multiple photon emission and KKMC with second order matrix element and exponentiation. In the left frame the invariant mass of the $\mu^+ \mu^-$ pair; $SDP=0.00142$. In the right frame the invariant mass of the $\gamma\gamma$; $SDP=0.00293$. The fraction of events with two hard photons was $1.2659 \pm 0.0011\%$ for KKMC and $1.2868 \pm 0.0011\%$ for PHOTOS. **BENCHMARK FIGURE to be reproduced by user.**

Reference root files available from web page of slide 7.

3 Decay Channel: $Z^0 \rightarrow \mu^- \mu^+ \gamma \gamma$

Number of events from generator 1: 1265886

Number of events from generator 2: 1262625



Z. Was

- Because (we will come to that later) event record contains tree-like structure one can think of a QED final state bremsstrahlung as an algorithm for the replacement of one decay vertex with another one.
- The existing vertex is de-constructed into
 - kinematical variables of the original process (for Z or W decays it is $\cos \Theta$ and ϕ)
 - factor for the denominator of the future weight: no bremsstrahlung Matrix and phase space Jacobian.
- In short, content of the event record is used as a generator for $\cos \Theta$ and ϕ variables, no more than that.
- Of course the question is, if it is known:
 - matrix element,
 - frame orientation,
 - vertex identification.
- All this is decisive for quality of algorithm functioning.

Phase Space: must be exact to discuss matrix elements

Orthodox exact Lorentz-invariant phase space (*Lips*) is in use in PHOTOS!

$$\begin{aligned}
 dLips_{n+1}(P) &= \\
 & \frac{d^3 k_1}{2k_1^0 (2\pi)^3} \cdots \frac{d^3 k_n}{2k_n^0 (2\pi)^3} \frac{d^3 q}{2q^0 (2\pi)^3} (2\pi)^4 \delta^4 \left(P - \sum_1^n k_i - q \right) \\
 &= d^4 p \delta^4 (P - p - q) \frac{d^3 q}{2q^0 (2\pi)^3} \frac{d^3 k_1}{2k_1^0 (2\pi)^3} \cdots \frac{d^3 k_n}{2k_n^0 (2\pi)^3} (2\pi)^4 \delta^4 \left(p - \sum_1^n k_i \right) \\
 &= d^4 p \delta^4 (P - p - q) \frac{d^3 q}{2q^0 (2\pi)^3} dLips_n(p \rightarrow k_1 \dots k_n).
 \end{aligned}$$

Integration variables, the four-vector p , compensated with $\delta^4(p - \sum_1^n k_i)$, and another integration variable M_1 compensated with $\delta(p^2 - M_1^2)$ are introduced.

Phase Space Formula of Photos

$$dLips_{n+1}(P \rightarrow k_1 \dots k_n, k_{n+1}) = dLips_n^{+1 \text{ tangent}} \times W_n^{n+1},$$

$$dLips_n^{+1 \text{ tangent}} = dk_\gamma d \cos \theta d\phi \times dLips_n(P \rightarrow \bar{k}_1 \dots \bar{k}_n),$$

$$\{k_1, \dots, k_{n+1}\} = \mathbf{T}(k_\gamma, \theta, \phi, \{\bar{k}_1, \dots, \bar{k}_n\}). \quad (1)$$

1. One can verify that if $dLips_n(P)$ was exact, then this formula lead to exact parametrization of $dLips_{n+1}(P)$
2. Practical implementation: Take completely constructed n-body phase space point (event).
3. Reconstruct coordinate variables, any parametrization can be used.
4. Construct new kinematical configuration from those variables and $k_\gamma \theta \phi$.
5. **Forget about temporary $k_\gamma \theta \phi$. Now, only weight and new four vectors count.**
6. A lot depend on \mathbf{T} . Options depend on matrix element: must tangent at singularities. Simultaneous use of several \mathbf{T} is necessary/convenient if more than one charge is present in final state.

Phase Space: (main formula)

If we choose

$$G_n : M_{2\dots n}^2, \theta_1, \phi_1, M_{3\dots n}^2, \theta_2, \phi_2, \dots, \theta_{n-1}, \phi_{n-1} \rightarrow \bar{k}_1 \dots \bar{k}_n \quad (2)$$

and

$$G_{n+1} : k_\gamma, \theta, \phi, M_{2\dots n}^2, \theta_1, \phi_1, M_{3\dots n}^2, \theta_2, \phi_2, \dots, \theta_{n-1}, \phi_{n-1} \rightarrow k_1 \dots k_n, k_{n+1} \quad (3)$$

then

$$\mathbf{T} = G_{n+1}(k_\gamma, \theta, \phi, G_n^{-1}(\bar{k}_1, \dots, \bar{k}_n)). \quad (4)$$

The ratio of the Jacobians form the phase space weight W_n^{n+1} for the transformation. Such solution is universal and valid for any choice of G 's. However, G_{n+1} and G_n has to match matrix element, otherwise algorithm will be inefficient (factor 10^{10} ...).

In case of PHOTOS G_n 's

$$W_n^{n+1} = k_\gamma \frac{1}{2(2\pi)^3} \times \frac{\lambda^{1/2}(1, m_1^2/M_{1\dots n}^2, M_{2\dots n}^2/M_{1\dots n}^2)}{\lambda^{1/2}(1, m_1^2/M^2, M_{2\dots n}^2/M^2)}, \quad (5)$$

Phase Space: (multiply iterated)

By iteration, we can generalize formula (1) and add l particles:

$$\begin{aligned}
 dLips_{n+l}(P \rightarrow k_1 \dots k_n, k_{n+1} \dots k_{n+l}) &= \frac{1}{l!} \prod_{i=1}^l \left[dk_{\gamma_i} d \cos \theta_{\gamma_i} d\phi_{\gamma_i} W_{n+i-1}^{n+i} \right] \\
 &\times dLips_n(P \rightarrow \bar{k}_1 \dots \bar{k}_n), \\
 \{k_1, \dots, k_{n+l}\} &= \mathbf{T}(k_{\gamma_l}, \theta_{\gamma_l}, \phi_{\gamma_l}, \mathbf{T}(\dots, \mathbf{T}(k_{\gamma_1}, \theta_{\gamma_1}, \phi_{\gamma_1}, \{\bar{k}_1, \dots, \bar{k}_n\}) \dots).
 \end{aligned} \tag{6}$$

Note that variables $k_{\gamma_m}, \theta_{\gamma_m}, \phi_{\gamma_m}$ are used at a time of the m -th step of iteration only, and are not needed elsewhere in construction of the physical phase space; the same is true for invariants and angles $M_{2 \dots n}^2, \theta_1, \phi_1, \dots, \theta_{n-1}, \phi_{n-1} \rightarrow \bar{k}_1 \dots \bar{k}_n$ of (2,3), which are also redefined at each step of the iteration. Also intermediate steps require explicit construction of temporary $\bar{k}'_1 \dots \bar{k}'_n \dots \bar{k}'_{n+m}$, statistical factor $\frac{1}{l!}$ added.

We have **exact distribution of weighted** events over l and $n + l$ body phase spaces.

Crude Distribution for multiple emission

If we add arbitrary factors $f(k_{\gamma_i}, \theta_{\gamma_i}, \phi_{\gamma_i})$ and sum over l we obtain:

$$\begin{aligned} & \sum_{l=0} \exp(-F) \frac{1}{l!} \prod_{i=1}^l f(k_{\gamma_i}, \theta_{\gamma_i}, \phi_{\gamma_i}) dLips_{n+l}(P \rightarrow k_1 \dots k_n, k_{n+1} \dots k_{n+l}) = \\ & \sum_{l=0} \exp(-F) \frac{1}{l!} \prod_{i=1}^l \left[f(k_{\gamma_i}, \theta_{\gamma_i}, \phi_{\gamma_i}) dk_{\gamma_i} d \cos \theta_{\gamma_i} d\phi_{\gamma_i} W_{n+i-1}^{n+i} \right] \times \\ & dLips_n(P \rightarrow \bar{k}_1 \dots \bar{k}_n), \tag{7} \\ & \{k_1, \dots, k_{n+l}\} = \mathbf{T}(k_{\gamma_l}, \theta_{\gamma_l}, \phi_{\gamma_l}, \mathbf{T}(\dots, \mathbf{T}(k_{\gamma_1}, \theta_{\gamma_1}, \phi_{\gamma_1}, \{\bar{k}_1, \dots, \bar{k}_n\}) \dots), \\ & F = \int_{k_{min}}^{k_{max}} dk_{\gamma} d \cos \theta_{\gamma} d\phi_{\gamma} f(k_{\gamma}, \theta_{\gamma}, \phi_{\gamma}). \end{aligned}$$

- The **Green** parts of rhs. alone, give crude distribution over tangent space (orthogonal set of variables k_i, θ_i, ϕ_i).

3. Toward n Poissonian distribution for tangent-space of independent photons. 20

- Factors f (W ' ignored) must be integrable over coordinates. Regulators of singularities necessary, but simple.
- If we request from infrared regulators, f and F that

$$\sigma_{tangent} = 1 = \sum_{l=0} \exp(-F) \frac{1}{l!} \prod_{i=1}^l \left[f(k_{\gamma_i}, \theta_{\gamma_i}, \phi_{\gamma_i}) dk_{\gamma_i} d \cos \theta_{\gamma_i} d\phi_{\gamma_i} \right]$$

we get Poissonian distribution in l .

- Sum rules originating from perturbative approach (KLM theorem) are necessary to incorporate dominant part of virtual corrections, into the scheme. We get Monte Carlo solution of PHOTOS type.
- For that to work, real emission and virtual corrections need to be calculated and their factorization properties analyzed. Choice for f and G are fixed from that.
- If such conditions are fulfilled construction of Monte Carlo algorithm is prepared.
- Truncate $\sigma_{tangent} |_{\mathcal{O}(\alpha), \mathcal{O}(\alpha^2)}$, \rightarrow phase space in single/double photon mode.

- Fully differential single photon emission formula in Z decay (F. Berends et al. 1982) reads:

$$X_f = \frac{Q'^2 \alpha (1 - \Delta)}{4\pi^2 s} s^2 \left\{ \frac{1}{(k'_+ k'_-)} \left[\frac{d\sigma_B}{d\Omega}(s, t, u') + \frac{d\sigma_B}{d\Omega}(s, t', u) \right] \right\}$$

- Variables in use:

$$s = 2p_+ \cdot p_-, \quad s' = 2q_+ \cdot q_-, \quad t = 2p_+ \cdot q_+, \quad t' = 2p_+ \cdot q_-,$$

$$u = 2p_+ \cdot q_-, \quad u' = 2q_- \cdot q_+, \quad k'_\pm = q_\pm \cdot k, \quad x_k = 2E_\gamma / \sqrt{s}$$

- The Δ term is responsible for final state mass dependent terms, p_+, p_-, q_+, q_-, k denote four-momenta of incoming positron, electron beams, outgoing muons and bremsstrahlung photon.
- Factorization of first order matrix element and fully differential distribution breaks at the level $\frac{\alpha^2}{\pi^2} \simeq 10^{-4}$

- after trivial manipulation it can be written as:

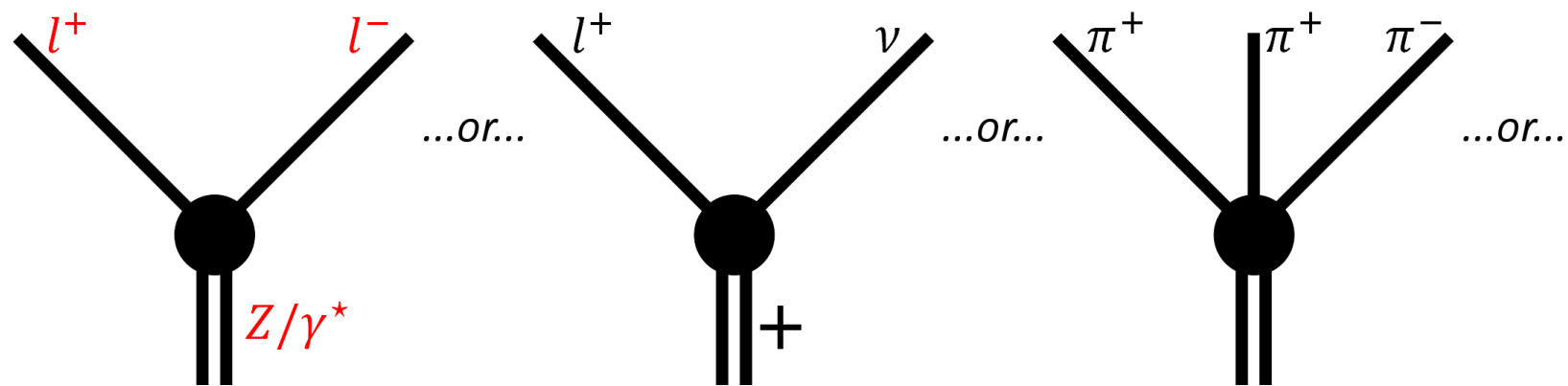
$$X_f = \frac{Q'^2 \alpha (1 - \Delta)}{4\pi^2 s} s^2 \left\{ \frac{1}{(k'_+ + k'_-)} \frac{1}{k'_-} \left[\frac{d\sigma_B}{d\Omega}(s, t, u') + \frac{d\sigma_B}{d\Omega}(s, t', u) \right] + \frac{1}{(k'_+ + k'_-)} \frac{1}{k'_+} \left[\frac{d\sigma_B}{d\Omega}(s, t, u') + \frac{d\sigma_B}{d\Omega}(s, t', u) \right] \right\}$$

- In PHOTOS the following kernel is used (decay channel, decay particle orientation, independent, **essential: universal interference *wt* introduced too**):

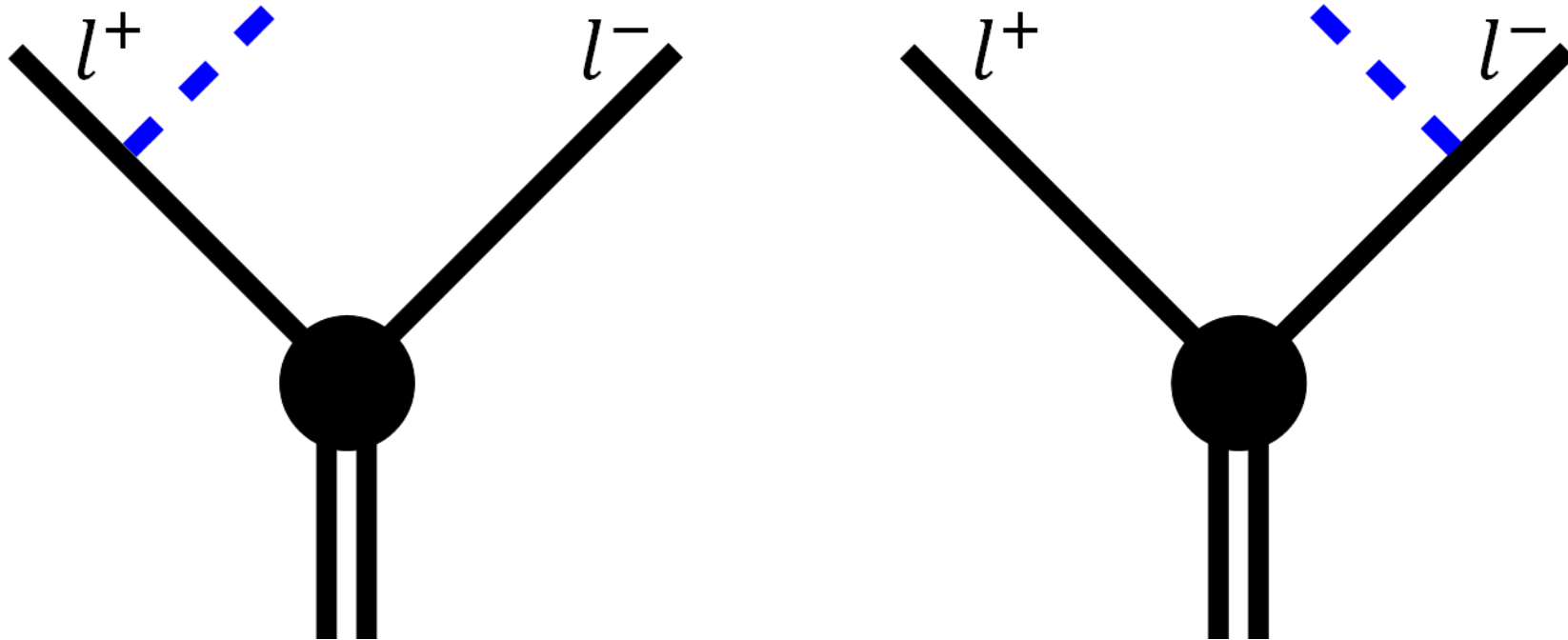
$$X_f^{PHOTOS} = \frac{Q'^2 \alpha (1 - \Delta)}{4\pi^2 s} s^2 \left\{ \frac{1}{k'_+ + k'_-} \frac{1}{k'_-} \left[(1 + (1 - x_k)^2) \frac{d\sigma_B}{d\Omega} \left(s, \frac{s(1 - \cos \Theta_+)}{2}, \frac{s(1 + \cos \Theta_+)}{2} \right) \right] \frac{(1 + \beta \cos \Theta_\gamma)}{2} + \frac{1}{k'_+ + k'_-} \frac{1}{k'_+} \left[(1 + (1 - x_k)^2) \frac{d\sigma_B}{d\Omega} \left(s, \frac{s(1 - \cos \Theta_-)}{2}, \frac{s(1 + \cos \Theta_-)}{2} \right) \right] \frac{(1 - \beta \cos \Theta_\gamma)}{2} \right\}$$

where : $\Theta_+ = \angle(p_+, q_+)$, $\Theta_- = \angle(p_-, q_-)$

$\Theta_\gamma = \angle(\gamma, \mu^-)$ are defined in (μ^+, μ^-) -pair rest frame



- The formula which we had on previous slide could be constructed because the Born level matrix element (and resulting Born level distribution) relates with the one of first order in α_{QED} through convolution of positively defined function (I will use it as emission kernel) (Berends Kleiss Jadach 1982).
- Does such convolution hold for other processes, even if we are concerned with the first order only?
- Paper by R. Kleiss from 1992 tells us that it will not hold at level of $(\frac{\alpha}{\pi})^2 \simeq 10^{-5}$.
- Comment, these properties are important for all variants of NLO factorizations.
- All these issues can be solved with studies of matrix elements only.



- *Structure of singularities for the first order corrections to decay of Z/γ^* which we will use as an example.*
- *Two kinematical branches need to be taken into account.*
- *Fortunately kinematical parametrizations for the two branches have identical phase space Jacobians. It simplifies tasks for multiphoton configurations.*

$$M^\alpha =$$

The image shows four Feynman diagrams representing FSR in Z/γ^* decays. Each diagram consists of a central vertex (black circle) with two incoming lines (double lines) and two outgoing lines. The first two diagrams show a wavy photon line attached to the outgoing lines, with labels l^+ and l^- on the lines. The last two diagrams show a wavy photon line attached to the incoming lines.

- Feynman diagrams for FSR in Z/γ^* decays
- Out of the **first two** diagrams distribution for Z/γ decay was obtained.
- Other two diagrams appear e.g. in scalar QED, and/or in decays of W 's or B mesons.
- Let us look into sub-structure of these amplitudes.

Matrix Element Z/γ^ decay, (formalism \sim Kleiss-Stirling methods):*

-

$$I = I^A + I^B + I^C$$

-

$$I = \mathcal{J} \left[\left(\frac{p \cdot e_1}{p \cdot k_1} - \frac{q \cdot e_1}{q \cdot k_1} \right) \right] - \left[\frac{1}{2} \frac{\not{e}_1 \not{k}_1}{p \cdot k_1} \right] \mathcal{J} + \mathcal{J} \left[\frac{1}{2} \frac{\not{e}_1 \not{k}_1}{q \cdot k_1} \right]$$

- Decomposes into 3 parts. Each is independently gauge invariant, valid for “any” \mathcal{J} .
- Only $|I^A|^2$ contributes to infrared singularities.
- Terms I^B and I^C contribute to collinear big logarithms.
- We could expect another term I^D which would not contribute neither to collinear nor soft divergent/large logarithms (once integration is performed)

structure of singularities apparent already at amplitude level

What happens for other decays

1. $W \rightarrow l\nu_l\gamma$: I^A , I^B and I^D dependent on electroweak calculation scheme.
2. $B^0 \rightarrow \pi^+K^-\gamma$: I^A only
3. $B^+ \rightarrow \pi^0K^+\gamma$: I^A only
4. $\gamma^* \rightarrow \pi^+\pi^-\gamma$: I^A , and I^D
5. $\tau^+ \rightarrow \pi^+\nu_\tau\gamma$: I^A and I^D
6. ...

It is important that in all cases, and not only for processes of QED, amplitudes can be constructed from the same building blocks.

These properties of amplitudes translate into properties of distributions and that is why exact PHOTOS algorithm for single photon emission can be constructed.

If non dominant terms can be neglected algorithm simplifies and process dependent weights can be replaced by the ones depending on charges and spins of outgoing particles.

Single emission

1. Solution for single emission works perfect.
2. Technical precision controlled to precision better than statistical error of 100 Mevts.
3. An example where interference between emission from two charged lines is hidden in exact process dependent kernel, but must be added if basically identical one is used.
4. Web page with multitude of automated tests (RECOMENDATION: to be repeated after installation in collaboration software):
<http://mc-tester.web.cern.ch/MC-TESTER/>
5. Let us go to iteration, used in solution for double and multiple photon emission modes.

(4) Implementation of matrix elements. Multiple emissions 29

Elementary test of principle

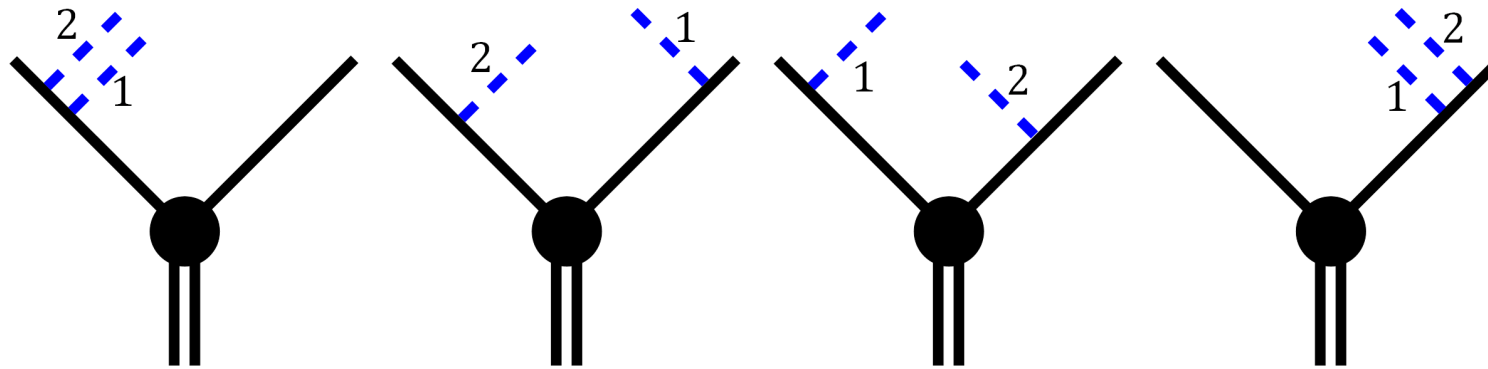
- Do PHOTOS generate the LL contribution to lepton spectra?
- Formal solution of QED evolution equation can be written as:

$$D(x, \beta_{ch}) = \delta(1-x) + \beta_{ch} P(x) + \frac{1}{2!} \beta_{ch}^2 \{P \times P\}(x) + \frac{1}{3!} \beta_{ch}^3 \{P \times P \times P\}(x) + \dots \quad (8)$$

where $P(x) = \delta(1-x)(\ln \varepsilon + 3/4) + \Theta(1-x-\varepsilon) \frac{1}{x} (1+x^2)/(1-x)$
and $\{P \times P\}(x) = \int_0^1 dx_1 \int_0^1 dx_2 \delta(x - x_1 x_2) P(x_1) P(x_2)$.

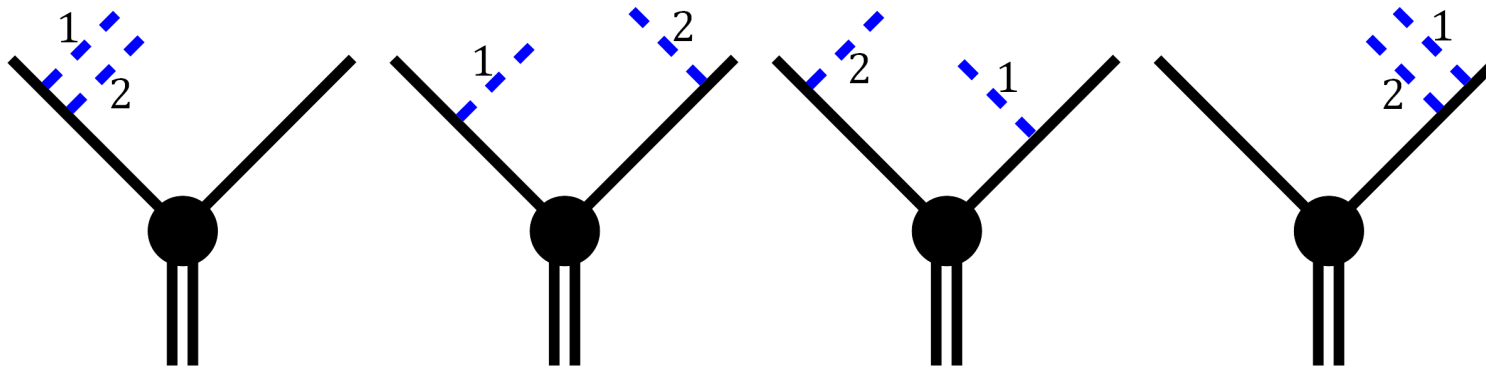
- In LL contributing regions, phase space Jacobian's of PHOTOS trivialize (CPC 1994). and the expression given above is obtained in a straightforward manner. In fact for each of the outgoing charged lines simultaneously.
- But it is only a limit! **PHOTOS treat phase space corners exactly.** We had to understand at spin amplitude, and exact distribution, levels why formula (8) work, keeping in mind what happens with amplitudes non leading parts.

(4) Implementation of matrix elements. Multiple emissions 30



- *To generate consecutive photons, PHOTOS simply iterates its single photon algorithm.*
- *Previously generated photons are treated as any other decay products.*
- *We generate photon 1 (each leg one after another)*
- *We include interference or matrix element weight*
- *And in the same way photon 2.*
- *previously generated photon(s) we remove, for matrix element calculation, from kinematical configuration, using reduction procedure.*
- *Iterative nature is very similar to solution for $D(x, \beta_{ch}) \times D(y, \beta_{ch})$, but except collinear limit, here, $x_1 x_2$ extends to 3 dimensions and as a consequence order of generating emissions matter $\hat{x}_1 \hat{x}_2 \neq \hat{x}_2 \hat{x}_1$. Also generating of x -es and y -es are affecting each other.*

(4) Implementation of matrix elements. Multiple emissions 31



- *We can produce such point in phase space starting with generation of photon 2 and continuing with 1.*
- *Each of the two generation chains cover all phase space. There is no phase space ordering in use. Instead we have statistical factor $\frac{1}{i!}$ from phase space*
- *Such solution must be confronted with distributions obtained from matrix elements.*
- *Comparisons with distributions obtained from double and triple photon amplitudes were performed in 1994.*
- *Now let us look at properties of spin amplitudes.*

(4) Implementation of matrix elements. Multiple emissions 32

$$M^{\alpha^2} = \text{[Diagram 1]} + \text{[Diagram 2]} + (\dots)$$

The diagram shows the matrix element M^{α^2} as a sum of terms. The first term is a vertex with two outgoing fermion lines and two incoming fermion lines, with two photons (wavy lines) emitted from the vertex. The second term is similar, but the photons are emitted from the fermion lines. The third term is represented by three dots in parentheses, indicating further terms in the series.

- *We have to check if description given in two previous slides justifies with properties of spin amplitudes.*
- *Iterative algorithm? What with interferences of consecutive emissions?*
- *It is important to check if such properties are process dependent or generalize.*
- *My decade long work under leadership of S. Jadach on e^+e^- generators provided help.*
- *Is double photon emission amplitude build from terms we know from first order?*
- *From calculation it is clear that the structure of $Z/\gamma^* \rightarrow l^+l^- \gamma\gamma$ generalizes to other processes.*

(4) Implementation of matrix elements. Multiple emissions 33

Exact Matrix Element: $Z \rightarrow \mu^+ \mu^- \gamma \gamma$ written explicitly

- We use conventions from paper A. van Hameren, Z.W., EPJC 61 (2009) 33. Expressions are valid for any current J , (also for QCD part proportional to $\{T^A T^B\}$, T^A is for first T^B for second gluon).
- To get complete amplitude sum the gauge invariant parts, add spinors, eg. $\bar{u}(p)$ and $v(q)$; $k_1/k_2 e_1/e_2$ denotes momenta/polarizations for 1-st/2-nd photon/gluon. Factors of parts coincide with those of first order.

$$I_1^{\{1,2\}} = \frac{1}{2} J \left(\frac{p \cdot e_1}{p \cdot k_1} - \frac{q \cdot e_1}{q \cdot k_1} \right) \left(\frac{p \cdot e_2}{p \cdot k_2} - \frac{q \cdot e_2}{q \cdot k_2} \right) \quad \text{eikonal}$$

$$I_{2l}^{\{1,2\}} = -\frac{1}{4} \left[\left(\frac{p \cdot e_1}{p \cdot k_1} - \frac{q \cdot e_1}{q \cdot k_1} \right) \frac{\not{\epsilon}_2 \not{k}_2}{p \cdot k_2} + \left(\frac{p \cdot e_2}{p \cdot k_2} - \frac{q \cdot e_2}{q \cdot k_2} \right) \frac{\not{\epsilon}_1 \not{k}_1}{p \cdot k_1} \right] J \quad \beta_1$$

(4) Implementation of matrix elements. Multiple emissions 34

$$I_{2r}^{\{1,2\}} = \frac{1}{4} \mathcal{J} \left[\left(\frac{p \cdot e_1}{p \cdot k_1} - \frac{q \cdot e_1}{q \cdot k_1} \right) \frac{k_2 \not{\epsilon}_2}{q \cdot k_2} + \left(\frac{p \cdot e_2}{p \cdot k_2} - \frac{q \cdot e_2}{q \cdot k_2} \right) \frac{k_1 \not{\epsilon}_1}{q \cdot k_1} \right] \quad \beta_1$$

$$I_3^{\{1,2\}} = -\frac{1}{8} \left(\frac{\not{\epsilon}_1 k_1}{p \cdot k_1} \mathcal{J} \frac{k_2 \not{\epsilon}_2}{q \cdot k_2} + \frac{\not{\epsilon}_2 k_2}{p \cdot k_2} \mathcal{J} \frac{k_1 \not{\epsilon}_1}{q \cdot k_1} \right) \quad \text{start for } \beta_2 \dots$$

$$I_{4p}^{\{1,2\}} = \frac{1}{8} \frac{1}{p \cdot k_1 + p \cdot k_2 - k_1 \cdot k_2} \left(\frac{\not{\epsilon}_1 k_1 \not{\epsilon}_2 k_2}{p \cdot k_1} + \frac{\not{\epsilon}_2 k_2 \not{\epsilon}_1 k_1}{p \cdot k_2} \right) \mathcal{J}$$

$$I_{4q}^{\{1,2\}} = \frac{1}{8} \mathcal{J} \frac{1}{q \cdot k_1 + q \cdot k_2 - k_1 \cdot k_2} \left(\frac{k_2 \not{\epsilon}_2 k_1 \not{\epsilon}_1}{q \cdot k_1} + \frac{k_1 \not{\epsilon}_1 k_2 \not{\epsilon}_2}{q \cdot k_2} \right)$$

$$I_{5pA}^{\{1,2\}} = \frac{1}{2} \mathcal{J} \frac{k_1 \cdot k_2}{p \cdot k_1 + p \cdot k_2 - k_1 \cdot k_2} \left(\frac{p \cdot e_1}{p \cdot k_1} - \frac{k_2 \cdot e_1}{k_2 \cdot k_1} \right) \left(\frac{p \cdot e_2}{p \cdot k_2} - \frac{k_1 \cdot e_2}{k_1 \cdot k_2} \right)$$

$$I_{5pB}^{\{1,2\}} = -\frac{1}{2} \mathcal{J} \frac{1}{p \cdot k_1 + p \cdot k_2 - k_1 \cdot k_2} \left(\frac{k_1 \cdot e_2 k_2 \cdot e_1}{k_1 \cdot k_2} - e_1 \cdot e_2 \right)$$

$$I_{5qA}^{\{1,2\}} = \frac{1}{2} \mathcal{J} \frac{k_1 \cdot k_2}{q \cdot k_1 + q \cdot k_2 - k_1 \cdot k_2} \left(\frac{q \cdot e_1}{q \cdot k_1} - \frac{k_2 \cdot e_1}{k_2 \cdot k_1} \right) \left(\frac{q \cdot e_2}{q \cdot k_2} - \frac{k_1 \cdot e_2}{k_1 \cdot k_2} \right)$$

(4) Implementation of matrix elements. Multiple emissions 35

$$I_{5qB}^{\{1,2\}} = -\frac{1}{2} \not{J} \frac{1}{q \cdot k_1 + q \cdot k_2 - k_1 \cdot k_2} \left(\frac{k_1 \cdot e_2 k_2 \cdot e_1}{k_1 \cdot k_2} - e_1 \cdot e_2 \right)$$

$$I_{6B}^{\{1,2\}} = -\frac{1}{4} \frac{k_1 \cdot k_2}{p \cdot k_1 + p \cdot k_2 - k_1 \cdot k_2} \left[+ \left(\frac{p \cdot e_1}{p \cdot k_1} - \frac{k_2 \cdot e_1}{k_1 \cdot k_2} \right) \frac{\not{e}_2 \not{k}_2}{p \cdot k_2} + \left(\frac{p \cdot e_2}{p \cdot k_2} - \frac{k_1 \cdot e_2}{k_1 \cdot k_2} \right) \frac{\not{e}_1 \not{k}_1}{p \cdot k_1} \right] \not{J}$$

$$I_{7B}^{\{1,2\}} = -\frac{1}{4} \not{J} \frac{k_1 \cdot k_2}{q \cdot k_1 + q \cdot k_2 - k_1 \cdot k_2} \left[+ \left(\frac{q \cdot e_1}{q \cdot k_1} - \frac{k_2 \cdot e_1}{k_1 \cdot k_2} \right) \frac{\not{k}_2 \not{e}_2}{q \cdot k_2} + \left(\frac{q \cdot e_2}{q \cdot k_2} - \frac{k_1 \cdot e_2}{k_1 \cdot k_2} \right) \frac{\not{k}_1 \not{e}_1}{q \cdot k_1} \right]$$

- for **exponentiation** one use **separation** into 3 parts only.

- $I_3^{\{1,2\}}$, $I_{4p}^{\{1,2\}}$, $I_{4q}^{\{1,2\}}$ were studied to improve options for PHOTOS kernel iteration. Things are less transparent, concept of effective fermionic momenta is used in interpretation, eg. $u((p - k_1)_{long}) \bar{u}((p - k_1)_{long}) \simeq \not{p} - \not{k}_1$, this makes sense only in some limits, but separation is all over phase space. **We got what is necessary! Parts for each kinematical branch. In fact sub-structures for amplitudes for processes of other theories appear as well.**

- Separation of β_2 into parts: of no use. No match with singularities of QED.

(4) Implementation of matrix elements. Multiple emissions 36

Status

- PHOTOS feature complete exact phase space for multiphoton radiation. In contrary to KKMC it does not rely on conformal symmetry for the masses photons phase space, but explore projections from tangent space. Matching of singular regions essential **CW complexes for triangulation of phase space manifolds.**
- Double iteration algorithm: Internal loop over emitting particles external one over photons, that is why one can simultaneously control eikonal and collinear enhancements.
- Studies of single/double photon spin amplitudes were essential.
- Work with SANC by D. Bardin et al., for Z and W decays. Necessary to understand separation of electroweak corrections into genuine weak and QED ISR and FSR.
- Checks of matrix elements installation, <http://annapurna.ifj.edu.pl/~wasm/phNLO.htm>
- ...comparisons with KKMC to confirm technical precision. KKMC is the program used at LEP for 2 MeV precision level measurements of Z . KKMC is based on exclusive exponentiation and features second order matrix element for FSR. Agreement better than 0.1 % in experimental cuts (ATLAS CDF) between PHOTOS and KKMC was found.

(4) Implementation of matrix elements. Multiple emissions 37

Principles → tests → systematic errors.

- PHOTOS feature complete exact phase space for multiphoton radiation. Can be used from F77 (HEPEVT) or C++ (HepMC).
- Comparisons with KKMC; program used at LEP for 2 MeV level measurements of Z point to precision better than 0.2 % for PHOTOS running at LO order (any type of cuts) and much better for NLO option. High precision has to be demonstrated on distributions with experiment-like cuts.
- Comparisons with SANC started by D. Bardin, for Z and for W decay are consistent with that precision level. They are necessary to understand numerically separation of electroweak corrections into genuine weak and QED (FSR).
- But photonic bremsstrahlung is not all what is needed for QED FSR.
- *Pair emission, implementation possible, because of tangent space arrangements, implemented in 2017*
- *initial Final state interferences must be checked to claim precision better than 0.5 %!*

- PHOTOS is scanning event record. It assumes that it is a tree. Often it is not ...
- Once vertex is identified as appropriate (decay of particle or resonance). algorithm is activated and with certain probability extra photon(s) are added.
- 4-momenta, masses and flavours of decaying particle and its daughters are used
- For NLO, we need to know the mothers of the decaying particle.
- Later kinematic o Daughters of daughters are adjusted as well.
- Several checks are performed. Decay products have to be stable particles. There must be energy momentum conservation in the vertex. True particles must be present. No gluons etc. Unless we have introduced exceptions.
- This is complex and never ending story, as new types of event fills appear in unexpected times.
- Tomasz will present some results on interaction with you we had in the last few months.

Status of Photos++

- The current version of Photos++ v3.51 has been thoughtfully tested and is installed and validated by GENSER project.
- Physical content of Photos++ remains stable since June 2011, when the last electroweak corrections algorithm has been introduced.
- Since then, only technical changes were made. Thanks to user feedback, new options have been added, installation scripts have been adjusted and Photos++ has been prepared to work with new types of event record structures as well as compensate for some of the inconsistencies within event record.

Photos++ and I/O traps

With every new version of Photos++ comes an extensive number of test validating both physics and technical side of the project. However, the most significant technical problems can only be found when Photos++ acts on events provided by users.

Photos++ was designed to deal with such special cases with minimum technical difficulties. The hardest part is to determine the physical nature of such cases, how they should be processed and what influence do they have on the rest of the event record.

Below are some of the problems we were able to find thanks to user feedback:

- **numerical precision and mass of the electrons and muons** - Photos++ expects that particles have proper mass and four-momenta. An option compensating precision loss or faulty information (such as mass presented in TeV instead of GeV) has been introduced.

- **status codes and history entries** - event records often contain particles that do not describe the actual event, such as history entries or entries before/after processing by external tool. Such particles are indicated by different status code, and different experiments use their own set of status codes for such purposes. The option of ignoring specific status codes had to be introduced. An options to create history entries of particles before `Photos++` processing has been introduced as well.
- **unexpected event structures** - `FORTRAN Photos` was designed to work on tree structure. However, with time, event records allowed much wider flexibility and such structure was no longer sufficient. This poses a set of new problems; each of them must be carefully examined. In one of such cases, decay vertices with three mothers had been found, which `Photos++` cannot process correctly. In other case events where subsequent particles form a loop, were present. In the most basic example, two particles decay to number of daughters, while two of these daughters create another $2 \rightarrow X$ decay vertex. In some cases, this caused `Photos++` to incorrectly boost such daughters,

creating NaNs.

- **$pp \rightarrow t\bar{t}$ and self-decay vertices** - another problem was found when working with Pythia8. In case of $pp \rightarrow t\bar{t}$ process, for each decay product of $t\bar{t}$ Pythia8 introduces a self-decay vertex boosted to different frame than the original particles. Photos++ had to deal with it by finding out the correct frame to which photons had to be boosted. To retain the same behaviour as this of Pythia8, an additional self-decay vertex for photons added by Photos had to be introduced.
- **pomerons and their diffractive states** - while this was not the problem in FORTRAN, it was physically incorrect for Photos++ to work on pomerons and they had to be added to the list of particles ignored by Photos++.

All of the above problems has been analysed and solution has been introduced, but we would like to stretch that these problems could not have been found if not for the user feedback.

Thanks to this, number of new options for Event Record manipulation have been added:

- `Photos::createHistoryEntries(bool flag, int status)`
- `Photos::ignoreParticlesOfStatus(int status)`
- `Photos::forceMassFrom4Vector(bool flag)`
- `Photos::forceMassFromEventRecord(int pdgid)`
- `Photos::forceMass(int pdgid, double mass)`

Already previously available options used to control ambiguities of event record:

- `Photos::suppressBremForDecay(daughterCount, motherID, d1ID, d2ID, ...)`
- `Photos::suppressBremForDecay(0, motherID)`
- `Photos::suppressBremForBranch(daughterCount, motherID, d1ID, d2ID, ...)`
- `Photos::processParticle(...)`
- `Photos::processBranch(...)`
- `Photos::forceBremForBranch(daughterCount, motherID, d1ID, d2ID, ...)`
- `Photos::forceBremForBranch(0, motherID)`
- `Photos::suppressAll()`
- `Photos::initializeKinematicCorrections(int flag)`
- `Photos::setMomentumConservationThreshold(double momentum_conservation_threshold)`

- Formula of Mustraal from 1982 is not only for final state bremsstrahlung
- It is valid for the initial state as well.
- At present for evaluation of intermediate state spin state information on partons resulting with the intermediate $Z/W/\gamma^*$ spin state information from parton shower variables stored in event record is used.
- This can be improved, but expected precision gain is rather small.
- This would be similar algorithm modification as discussed in Elzbieta talk.

Mustraal frame

[18] F. A. Berends, R. Kleiss, and S. Jadach, *Comput. Phys. Commun.* **29** (1983) 185–200.

Mustraal: Monte Carlo for $e^+ e^- \rightarrow \mu^+ \mu^- (\gamma)$

$$s = 2p_+ \cdot p_-, \quad t = 2p_+ \cdot q_+, \quad u = 2p_+ \cdot q_- \\ s' = 2q_+ \cdot q_-, \quad t' = 2p_- \cdot q_-, \quad u' = 2p_- \cdot q_+$$

$$\sigma_{\text{hard}} = \int d\tau (X_i + X_f + X_{\text{int}}),$$

The explicit forms of the three terms in σ_{hard} read:

$$X_i = \frac{Q^2 \alpha}{4\pi^2 s} \frac{1 - \Delta}{k_+ k_-} s'^2 \left[\frac{d\sigma^B}{d\Omega}(s', t, u) + \frac{d\sigma^B}{d\Omega}(s', t', u') \right], \quad (3.4)$$

$$X_f = \frac{Q'^2 \alpha}{4\pi^2 s} \frac{1 - \Delta'}{k'_+ k'_-} s^2 \left[\frac{d\sigma^B}{d\Omega}(s, t, u') + \frac{d\sigma^B}{d\Omega}(s, t', u) \right], \quad (3.5)$$

$$X_{\text{int}} = \frac{QQ'\alpha}{4\pi^2 s} W \frac{\alpha^2}{2ss'} \left[(u^2 + u'^2 + t^2 + t'^2) \tilde{f}(s, s') + \frac{1}{2}(u^2 + u'^2 - t^2 - t'^2) \tilde{g}(s, s') \right] \\ + \frac{QQ'\alpha^3}{4\pi^2 s} \frac{(s - s') M \Gamma}{k_+ k_- k'_+ k'_-} \epsilon_{\mu\nu\rho\sigma} p_+^\mu p_-^\nu q_+^\rho q_-^\sigma \left[\tilde{E}(s, s')(t^2 - t'^2) + \tilde{F}(s, s')(u^2 - u'^2) \right], \quad (3.6)$$

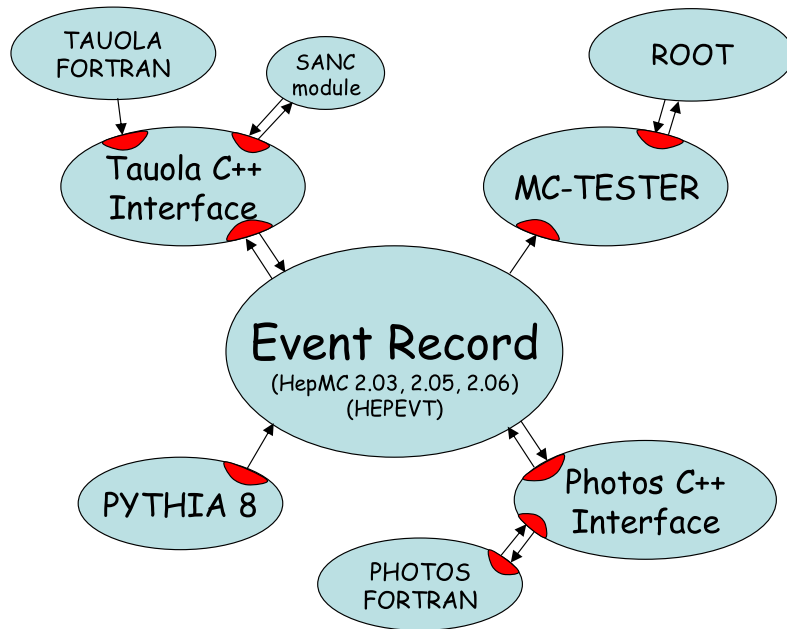
Resulting optimal frame used to minimise higher order corrections from initial state radiation in $e^+e^- \rightarrow Z/\gamma^* \rightarrow \mu \mu$ for algorithms of genuine EW corrections implementation in LEP time Monte Carlo's like Koral Z.

2

- QED final state bremsstrahlung does not form an undisputably separated from genuine weak and QCD physics phenomena.
- True, it is profitable to keep it separated/factorized, because of solvable infrared (also collinear) limit of QED, but it does not need to be so in every calculation scheme.
- Massive effort in our collaboration with D. Bardin group was devoted to make this possible, also for Monte Carlo matrix element input.
- In particular for the charged intermediate states (like W resonance). this required attention.
- Alternatively one has to go to much higher order of perturbation expansion for EW sector. Even 3-loops will bring then corrections of 1%.

- QED initial-final state interference is a complicated issue, because of initial state strong interactions.
- There are results demonstrating that for the semi-inclusive observables and around resonances interference effect is suppressed by the factor $\Gamma_X/M_X \simeq 1/30$. This is because of the resonances life-time.
- This time separation can be managed by selection cuts, because of uncertainty principle. Cuts may fix energy of particles thus enhance formation time, and damage production-decay separation.
- Cross-checks are necessary. KKMC-hh Phys.Rev. D94 (2016) no.7, 074006 may offer a good frame for such tests. [Note that KKMC-ee arXiv:1801.08611 offer benchmarks at \$10^{-4}\$ precision level.](#)
- This statement is independent on how progress on matching QED initial state photon emissions with parton showers, underlying event, MPI is progressing.

Simulation parts communicate through event record:



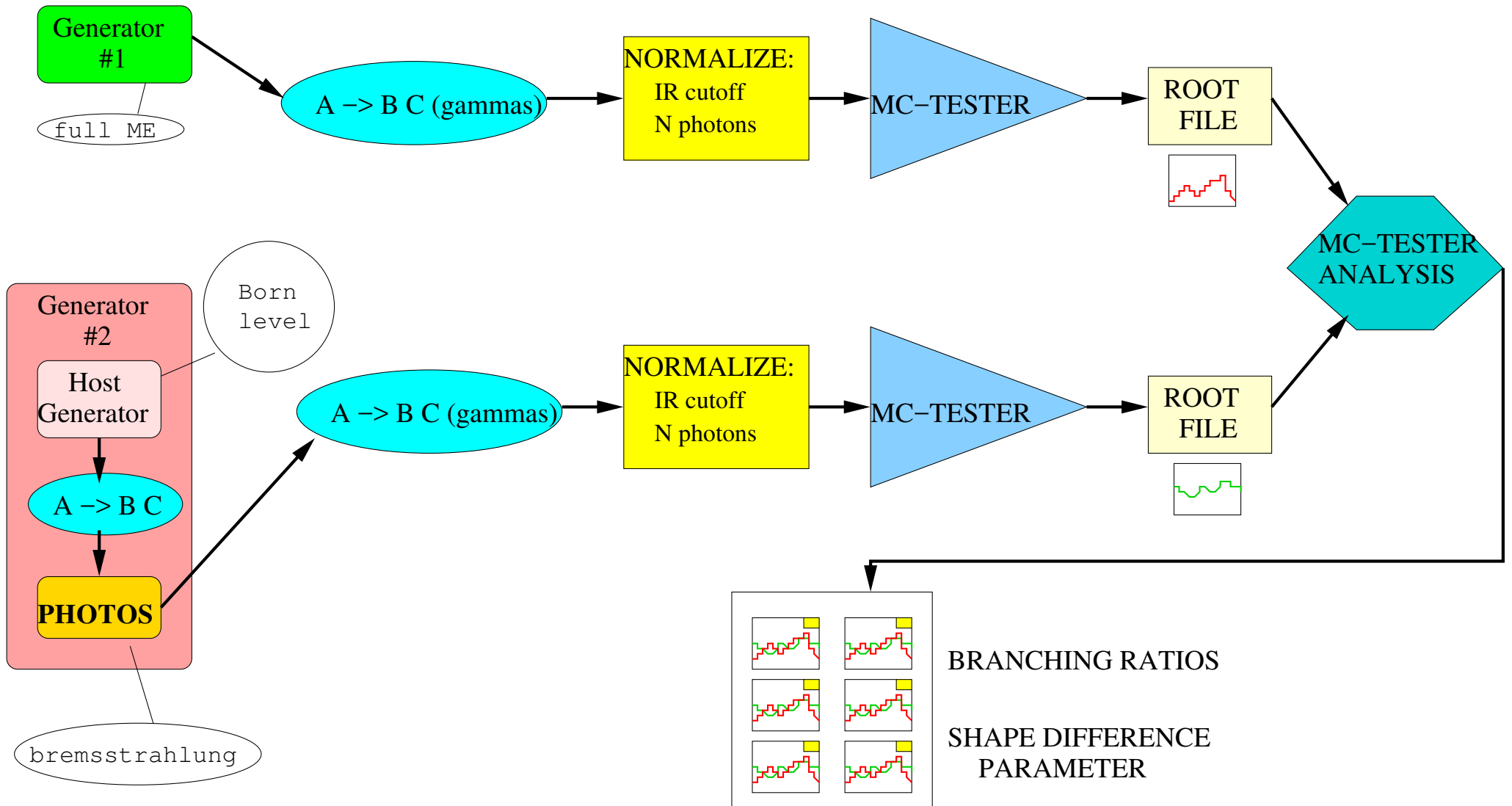
- Parts:

- hard process: (Born, weak, new physics),
- parton shower,
- τ decays
- QED bremsstrahlung
- High precision achieved
- Detector studies: acceptance, resolution lepton with or without photon.

Such organization requires:

- Good control of factorization (theory)
- Good understanding of tools on user side.

MC-TESTER to test PHOTOS/TAUOLA



- Large Booklets of KKMC PHOTOS comparisons for $w\bar{u} \rightarrow \mu^+ \mu^-$:

<http://annapurna.ifj.edu.pl/~wasm/results-nlo.ps> 169 pages

<http://annapurna.ifj.edu.pl/~wasm/results-lo.ps> 169 pages

Z virtuality 97.187 GeV (to get large A_{FB}). Selection cuts ; $p_T > 20 GeV$ for each lepton and pseudorapidity smaller than 2.4. Photon plots for $E_\gamma > 0.1$ GeV. Plots are (together with selection) in consecutive frames numbered by p_T and rapidity of the Z):

- LOG_{10} of the angle between closer lepton and photon (above threshold)
- LOG_{10} of $(1+c)/(1-c)$ where $c=c_1, c_2$ is cosine of the lepton angle with respect to z axis. For c_2 one bin histogram is defined. The plot of the ratio is used for visualization of normalization.

For photon angular distribution histograms of the ratios are also given. There are 6 figures for each combination of p_T and pseudorapidity.

Preliminary. 40 Mevts samples used. Confirm 0.2 % precision tag.

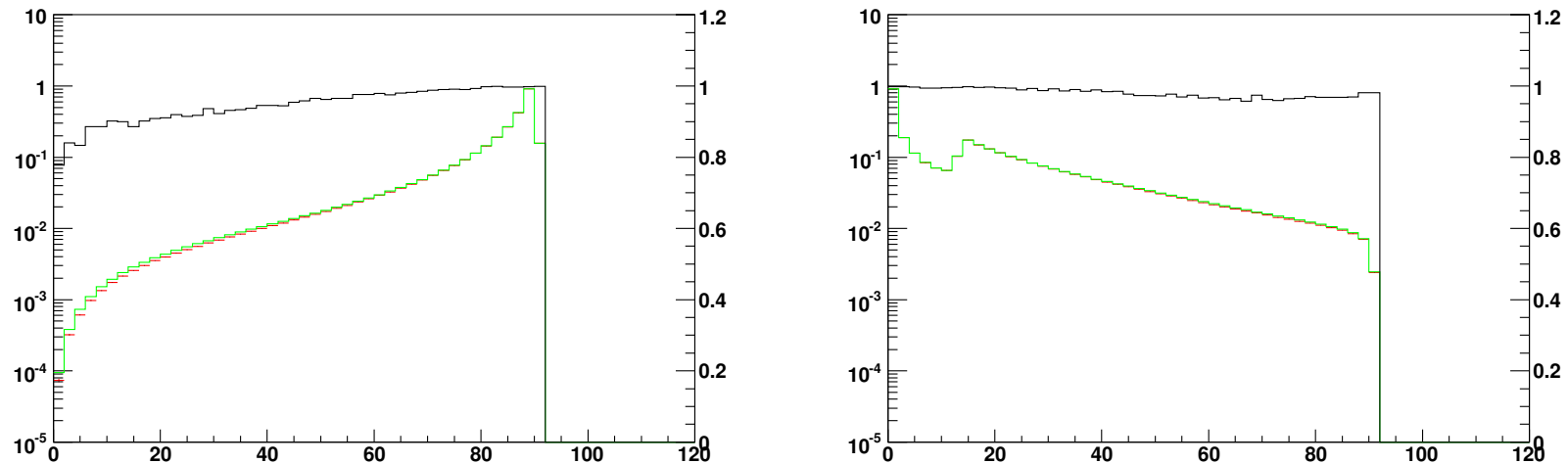


Figure 1: Comparison of standard PHOTOS and KORALZ for single photon emission. In the left frame the invariant mass of the $\mu^+ \mu^-$ pair; $SDP=0.00534$. In the right frame the invariant mass of $\mu^- \gamma$; $SDP=0.00296$. The histograms produced by the two programs (logarithmic scale) and their ratio (linear scale, black line) are plotted in both frames. The fraction of events with hard photon was $17.4863 \pm 0.0042\%$ for KORALZ and $17.6378 \pm 0.0042\%$ for PHOTOS. **BENCHMARK FIGURE** from our web page. To be reproduced.

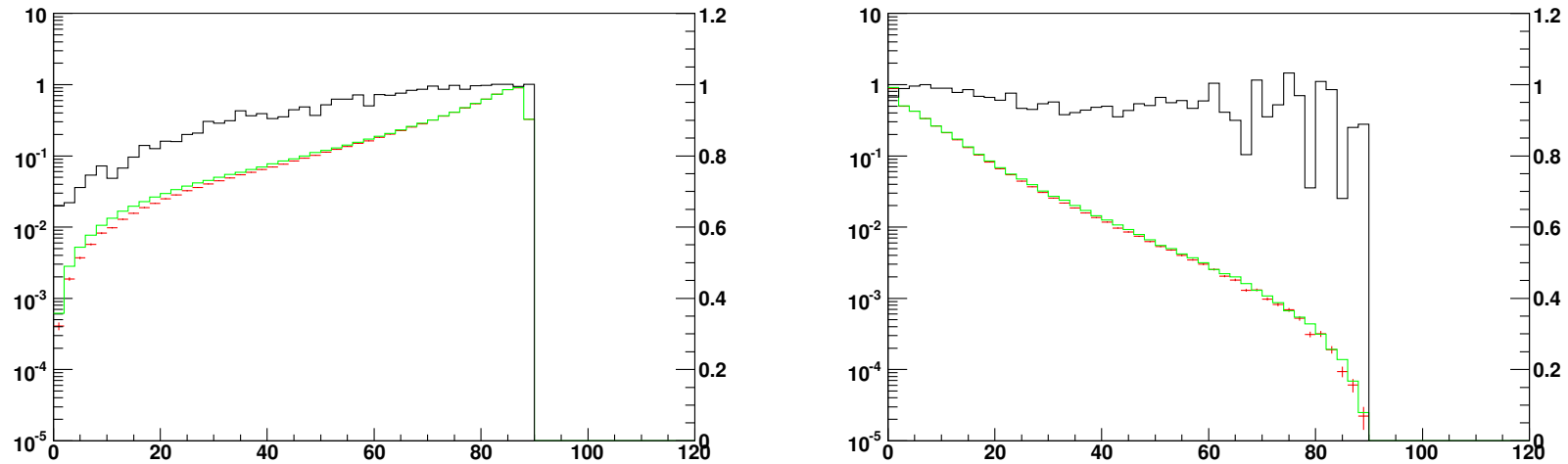


Figure 5: Comparisons of standard PHOTOS with multiple photon emission and KKMC with second order matrix element and exponentiation. In the left frame the invariant mass of the $\mu^+ \mu^-$ pair; SDP= 0.00918 (shape difference parameter). In the right frame the invariant mass of the $\gamma\gamma$ pair; SDP=0.00268. The fraction of events with two hard photons was $1.2659 \pm 0.0011\%$ for KKMC and $1.2952 \pm 0.0011\%$ for PHOTOS. **BENCHMARK FIGURE** from our web page. To be reproduced.

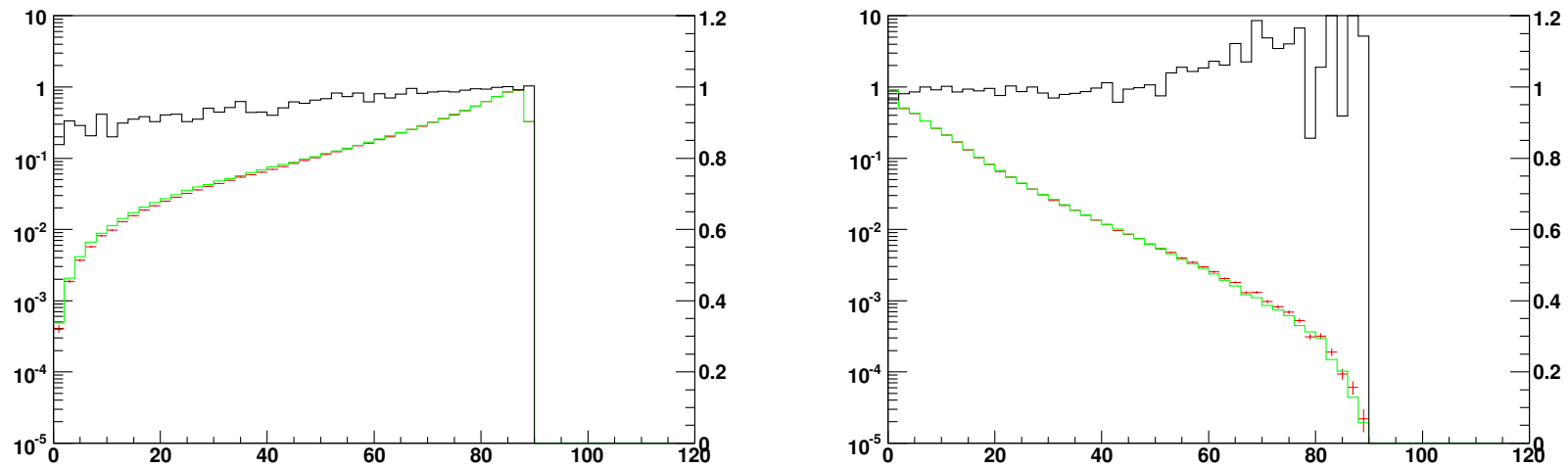
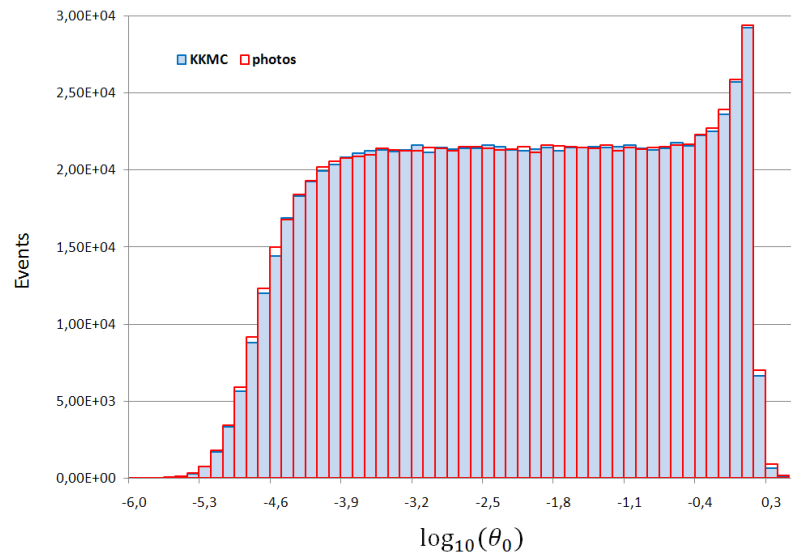


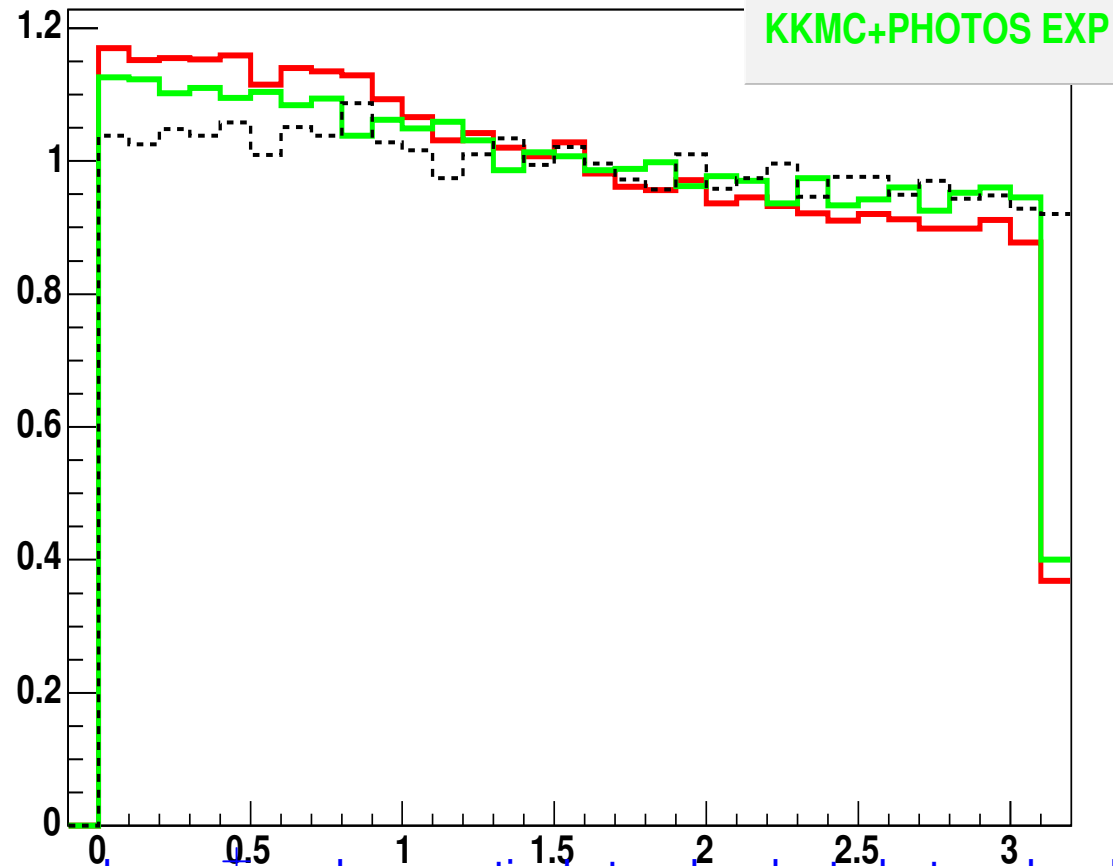
Figure 6: Comparisons of improved PHOTOS with multiple photon emission and KKMC with second order matrix element and exponentiation. In the left frame the invariant mass of the $\mu^+ \mu^-$ pair; $SDP= 0.00142$. In the right frame the invariant mass of the $\gamma\gamma$; $SDP=0.00293$. The fraction of events with two hard photons was $1.2659 \pm 0.0011\%$ for KKMC and $1.2868 \pm 0.0011\%$ for PHOTOS. **BENCHMARK FIGURE to be user reproduced.**



- $E_\gamma > 4 \text{ MeV}$. Angle with respect to closer fermion.

Acoplanarity distribution – Looks good

Acoplanarity



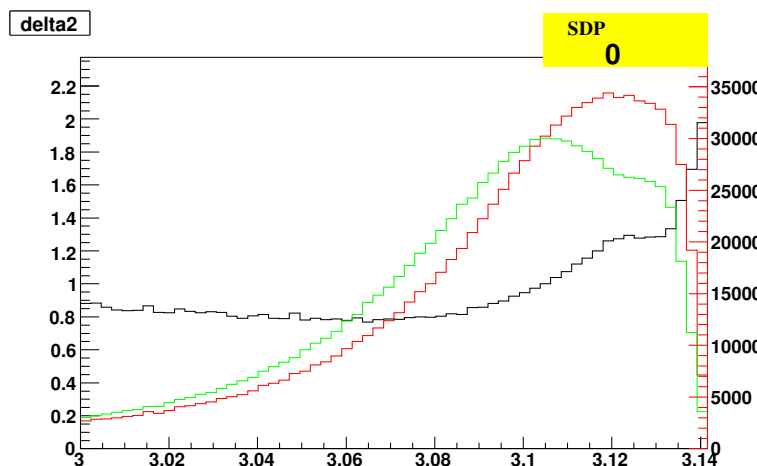
Two plane spanned on μ^+ and respectively two hardest photons localized in the same hemisphere as μ^+ . In exclusive exponentiation this asymmetry appears with second order matrix element only.

1. **I have presented mathematical and physics foundation of POHOTOS MC**
2. **I have given general description of the programme as well.**
3. **I have demonstrated the framework of tests and stressed that reliability rest on clear separation: what is phase-space what are ME.**
4. **Study of matrix element properties was essential.
For tests and for the design.**
5. **Framework for tests was presented too.**
6. **Points necessary for the precision improvements were listed.**

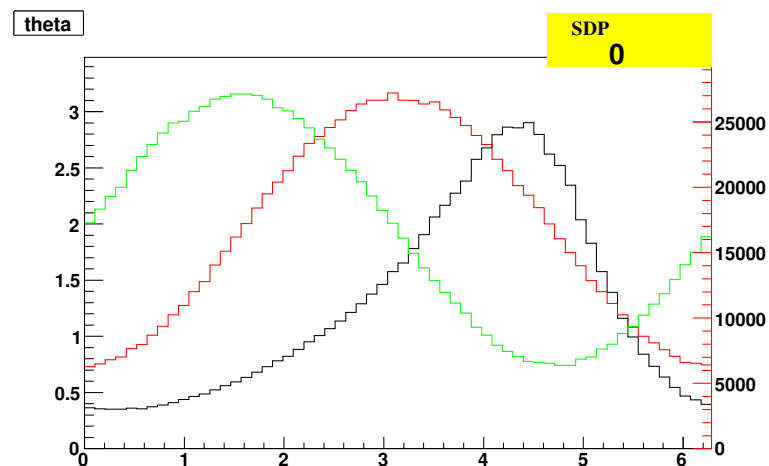
1. **Thanks to:**
 - (a) Mathematical considerations
 - (b) Calculation of spin amplitudes and evaluation of its parts
 - (c) Tests with semi-analytical results and results from other programs
2. **Evaluation of precision tag at 0.5-0.3 % was possible for Z and W decays.**
3. **Such statements are always observable dependent.**
4. **General scheme is the same as for benchmarks of KKMC**
5. **Evaluation of results for higher precision require common work with experiments.**
6. **Like it was the case for luminosity measurements at LEP. Granularity of detectors demands exclusive resummation.**
7. **Now it will be more difficult, because of need to factorize out difficult to control initial state strong interactions effects.**

1. Essential for the development of Photos iteration algorithm was work for the paper: *Hard photon bremsstrahlung in the process $pp \rightarrow Z^0/\gamma^* \rightarrow l^+l^-$: A background for the intermediate mass Higgs*, E. Richter-Was , Z.Phys. C64 (1994) 227-240
2. Important technical activity resulting with refinements of Photos iteration algorithm and its tests, took place in LAL.
3. Future improvements for precision, clear path:
 - (a) Mustraal Frame is direction for the better approximation of intermediate decaying state definition
 - (b) Missing effects like IFI interference
 - (c) Tests, including installation tests.
4. Final statement of precision requires comparison of results in real detection conditions.

Example: Distribution for Higgs parity



(a) $\pi^+ \pi^-$ acollinearity distribution ($\approx \pi$)



(b) $\pi^+ \pi^-$ acoplanarity distribution

Figure 1: Transverse spin observables for the H boson for $\tau^\pm \rightarrow \pi^\pm \nu_\tau$. Distributions are shown for scalar higgs (red), scalar-pseudoscalar higgs with mixing angle $\frac{\pi}{4}$ (green) and the ratio between the two (black).